Polydimethylsiloxane-polymethacrylate block copolymers tethering quaternary ammonium salt groups for antimicrobial coating

Xiaoshuai Qin, Yancai Li, Fang Zhou, Lixia Ren, Yunhui Zhao*, Xiaoyan Yuan

School of Materials Science and Engineering, and Tianjin Key Laboratory of Composite and Functional Materials, Tianjin University, Tianjin 300072, China

ARTICLE INFO

ABSTRACT

Block copolymers PDMS-*b*-PDMAEMA were synthesized via reversible addition-fragmentation chain transfer (RAFT) polymerization involving *N,N*-dimethylaminoethyl methacrylate (DMAEMA) by using poly(dimethylsiloxane) (PDMS) macro-chain transfer agent. And, the tertiary amino groups in PDMAEMA were quaternized with *n*-octyliodide to provide quaternary ammonium salts (QPDMAEMA). The well-defined copolymers generated composition variation and morphology evolvement on film surfaces, which were characterized by X-ray photoelectron spectroscopy, atomic force microscopy, and contact angle measurements. The results indicated that the enrichment of QPDMAEMA brought about lower elemental ratios of Si/N on the film surfaces. The surface morphologies evolved with the variations of QPDMAEMA content, and the variation trend of film roughness was exactly opposite to that of water contact angle hysteresis. With regard to structure-antimicrobial relationships, the copolymer films had more evident antimicrobial activity against Gram-positive, *Bacillus subtilis*, and the surfaces with hetero-geneous morphology and higher N^+ content presented better antimicrobial activity. The functionalized copolymers based PDMS and quaternary ammonium salts materials have the potential applications as antimicrobial coatings.

© 2014 Elsevier B.V. All rights reserved.

1. Introduction

The growth of bacteria is a particular contamination problem, which can lead to severe infections and diseases [1]. Great efforts have been devoted to develop materials with high antimicrobial performance. Antimicrobial polymers with diverse mechanisms, including quaternary ammonium salts (QAS), polymeric *N*-halamine, and host-defense peptide are of importance. Polymeric *N*-halamines possess the advantages of high efficiency, durability and rechargeability [2]. Host-defense peptides with sequence-specific structure can prevent bacteria from evolving resistance to the membrane-disruption mode [3]. QAS is the most popular antimicrobial polymeric material owing to its simple fabrication process and low cost, though it has relatively lower antimicrobial efficacy compared with polymeric *N*-halamines and antimicrobial peptides [4].

The antimicrobial activity of QAS related polymers was associated with complex factors, such as molecular weight, types of the counter anions, charge density, alkyl chain length and steric

hindrance of QAS, hydrophilic–hydrophobic balance, as well as bacteria species [5–9]. Some research groups indicated that QAS containing long alkyl chain substituent of at least 8 carbon atoms showed significant active biocides in water [6,7,10,11]. As well known, poly(*N,N*-dimethylaminoethyl methacrylate) (PDMAEMA) is one of the hydrophilic polymers containing tertiary amino groups, and can be further converted into positively charged polymer with quaternary ammonium salt groups (QPDMAEMA), which has been considered to be a promising polymeric antimicrobial agent [12–14]. A previous study reported antimicrobial polymeric brushes with high density cationic surfaces could effectively kill bacterial cells [15]. Tang's group [16] have studied ammonium containing PDMAEMA with natural rosin as the pendant groups (PDMAEMA-*g*-rosin), and indicated that conformation of hydrophobic group with particularly steric hindrance played an important role for antimicrobial efficacy. Moreover, it was reported that the QAS modification could enhance the mechanical properties of polysiloxane coatings [17].

From the aspect of application, poly(dimethylsiloxane) (PDMS) is one of the versatile candidates to integrate with QPDMAEMA, because of the good fouling-release performance, low surface energy and elastic modulus, as well as biocompatibility, optical transparency, and permeability [18–20]. Actually, there are several approaches utilized to endow PDMS with antimicrobial properties.

---

* Corresponding author at: School of Materials Science and Engineering, Tianjin University, Tianjin 300072, China. Tel.: +86 22 8740 1870; fax: +86 22 8740 1870.
E-mail address: zhaoyunhui@tju.edu.cn (Y. Zhao).

The facile techniques involve blending with various antimicrobial agents [6,21,22], and chemical surface modification of PDMS material with preformed polymers [23–25]. The drawbacks of these manipulations are that they cannot give long-term protection under adverse conditions and the modified surface of PDMS could be transformed into a brittle silica-like layer [26–28]. The available approach is based on constructing copolymers containing antimicrobial functional groups in side chains to tailor brush structures [8,29]. The controlled polymerizations, such as atom transfer radical polymerization (ATRP) [30] and RAFT polymerization [31], are often used to synthesize the target copolymers for antimicrobial purpose. Due to the high flexibility of PDMS chains, the QAS-tethered polysiloxane may readily interact with bacteria, acting not only on the surface but also in bulk, which would prevent the bacteria from colonizing crevices as well as defects of other materials [8].

For the purpose of finding an economic and practical biomedical antibacterial coating, in this study, a series of block copolymers with different content of QPDMAEMA were synthesized via RAFT polymerization and quaternization, taking the effects of charge density and molecular weight on antimicrobial efficiency into account. PDMS was used as macro chain transfer agent (PDMS-CTA) with low surface energy and biocompatibility available, while QPDMAEMA was designated to fulfill the antimicrobial function. The well-defined structure of copolymers endowed greater insight into microphase separation and the resulting antimicrobial activity, which could generate special composition and unique morphology on film surfaces. These block copolymer films were characterized by X-ray photoelectron spectroscopy (XPS), atomic force microscopy (AFM), and contact angle measurements. With regard to structure-antimicrobial relationships, the antimicrobial activity of the copolymers against Gram-positive and Gram-negative bacteria was preliminarily investigated.

2. Experimental

2.1. Materials

α-Hydride-terminated polydimethylsiloxane (PDMS-H, M_n = 8000 g/mol) was purchased from Hangzhou Silong Material Technology Co., Ltd., China. 2-(Allyloxy)ethanol, platinum(0)-1,3-divinyl-1,1,3,3-tetramethyldisiloxane complex solution in xylene (Pt ∼ 2%), 4-(dimethylamino)pyridine (DMAP, 99%) and N,N-dicyclohexylcarbodiimide (DCC) were purchased from Sigma-Aldrich. Hydroxyl-terminated polydimethylsiloxane (PDMS-OH) was synthesized from α-hydride-terminated polydimethylsiloxane according to the literature [32]. 4-Cyanopentanoic acid dithiobenzoate (CAD) was synthesized referring to the previous report [33]. PDMS-CTA was obtained according to the literatures [34,35]. N,N-dimethylaminoethyl methacrylate (DMAEMA) (Aldrich, 98%) and hydroxyethyl methacrylate (HEMA) (Tianjin Kemiou Chemical Reagent Co., China) were purified by passing the monomer through basic alumina column.

N-octyliodide was obtained from Alfa Aesar and used as received. Azobis(isobutyronitrile) (AIBN, Aldrich, 99%) was recrystallized from ethanol and dried. Hexamethylene diisocyanate (HDI) was purchased from Bayer AG., Germany. Gram-positive bacteria (Bacillus subtilis) and Gram-negative bacteria (Escherichia coli) were supplied from Hebei University of Science & Technology, China, and were incubated at 4 °C on nutrient agar plates.

2.2. Synthesis of PDMS-b-QPDMAEMA block copolymers

The synthesis procedure for PDMS-b-QPDMAEMA is described in Scheme 1. RAFT polymerization was conducted in a 50 mL dry three necked flask equipped with a magnetic stirrer. In a typical reaction, DMAEMA (0.942 g, 6 mmol), AIBN (0.0028 g, 0.017 mmol) and PDMS-CTA (1.008 g, 0.12 mmol) were dissolved in toluene (0.95 g). In addition, a certain amount of HEMA was added for crosslinking. The solution was then degassed to remove oxygen, and polymerization was carried out under stirring in water bath at 65 °C for 12 h. The reaction was terminated and quenched to 0 °C, and the crude products were diluted and dialyzed against methanol over 48 h. After dialysis, the solvent was removed by rotary evaporator and the copolymer was dried under high vacuum for 24 h at room temperature to yield a pink product. Block copolymers with different contents were synthesized in the same manner (Table 1). ^{1}H NMR (500 MHz, CDCl$_3$) d (ppm): 0.07 (6nH, m, C$_4$H$_9$(Si(CH_3)$_2$)$_n$), 0.91–1.06 (3H, s, CH$_2$C(CH_3)S), 1.80–1.90 (2H, s, CH_2C(CH$_3$)S), 2.32 (6H, s, CH$_2$N(CH_3)$_2$), 2.58 (2H, t, CH_2N(CH$_3$)$_2$), 3.83 (2H, t, CH$_2$CH_2OH), 4.08 (2H, t, COOCH_2CH$_2$N).

Quaternization reactions were carried out in a 50 mL dry three-necked flask equipped with a magnetic stirrer. In a typical reaction, 0.99 g of PDMS-b-PDMAEMA (2.4 mmol of tertiary amine functional groups) was mixed with 0.864 g of n-octyliodide (3.6 mmol of iodide ions), then the reactants were dissolved in toluene/acetonitrile (w/w = 1:1) solvents, and the quaternization reaction was proceed at 70 °C for 32 h. A substantial increase in viscosity was observed as a result of the reaction. The product was precipitated by hexane four times. ^{1}H NMR (500 MHz, CDCl$_3$) d (ppm): 0.07 (6nH, m, C$_4$H$_9$(Si(CH_3)$_2$)$_n$), 0.91–1.06 (3H, s, CH$_2$C(CH_3)S), 1.39 (17H, m, (CH_2)$_7$CH_3), 1.80–1.90 (2H, s, CH_2C(CH$_3$)S), 3.47 (6H, s, CH$_2$N$^+$(CH_3)$_2$), 3.72 (2H, t, CH_2N$^+$(CH$_3$)$_2$), 4.08–4.15 (2H, t, COOCH_2CH$_2$N). It was estimated that all the tertiary amino groups have almost been transformed into QAS groups.

### 2.3. Preparation of the copolymer films

A certain amount of the obtained block copolymers and HDI were dissolved in acetonitrile to prepare copolymer solution (10 wt%). Then the solution (200 μL) was spin-coating (rotate speed 600 r/s for 6 s and 3000 r/s for 10 s) on clean aluminum sheet (2 cm × 2 cm). The solvent was evaporated at room temperature for 1 h before the samples were cured at 100 °C for 2 h. These films were used for the characterization of surface structure and antimicrobial performance testing.

Table 1
Conversion and relative molecular weight of the prepared block copolymers.

Sample[a]	^{1}H NMR		GPC		
	Conv. (%)	$M_{n, NMR}$ (kDa)	M_n (kDa)	M_w (kDa)	PDI
PDMS	–	8.0	9.3	11.8	1.27
PDMS-b-PDMAEMA$_{40}$[b]	80.0	15.2	12.7	16.0	1.25
PDMS-b-PDMAEMA$_{60}$	60.0	16.8	15.6	18.7	1.20
PDMS-b-PDMAEMA$_{80}$	56.0	20.1	18.9	23.0	1.22
PDMS-b-PDMAEMA$_{100}$	72.8	23.5	23.7	28.0	1.18

[a] Each sample of the block copolymers contained approximately 15 repeat units of HEMA estimated by ^{1}H NMR for crosslinking.
[b] Subscripts represented the numbers of repeat units for PDMAEMA estimated by ^{1}H NMR.
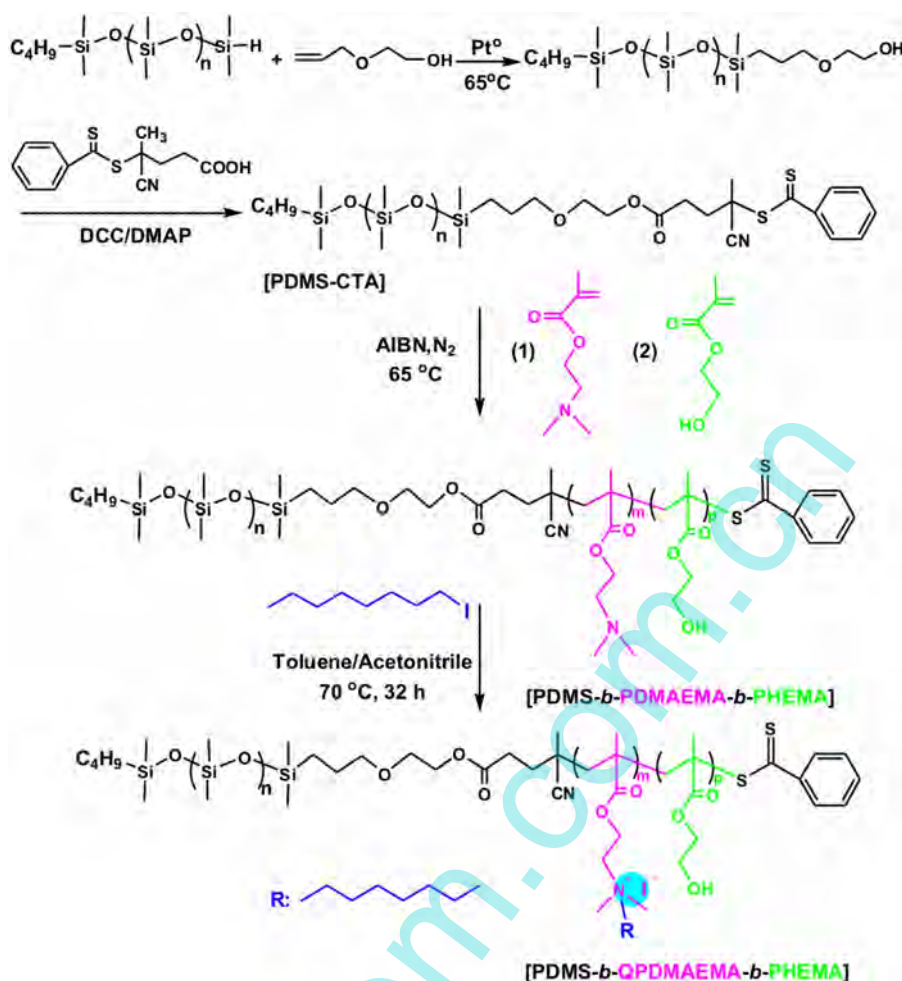
Scheme 1. Synthesis of PDMS-*b*-QPDMAEMA-*b*-PHEMA block copolymer.

2.4. Characterizations

^{1}H-nuclear magnetic resonance (^{1}H NMR) spectra were conducted on copolymers by a Bruker Avance 500 MHz at 25 °C. Deuterated chloroform (CDCl$_3$) was used as solvent, and all chemical shifts were reported in ppm (d).

Gel permeation chromatography (GPC) was equipped with Waters 1515 isocratic high performance liquid chromatography pump and Waters 2414 refractive index detector. Narrow polystyrene (PS) standards were used, and tetrahydrofuran was utilized as the eluent through a flow rate of 1.0 mL/min at 40 °C.

Differential scanning calorimetry (DSC) was carried out using a TA instrument (DSC F1 204) with an indium metal standard under a nitrogen atmosphere. Samples (5–6 mg) were heated from room temperature to 150 °C, and then cooled to −150 °C with heating and cooling rate of 30 °C min^{-1}. The samples were reheated to 150 °C with rate of 10 °C min^{-1}. The thermograms in the second heating run were recorded.

X-ray photoelectron spectroscopy (XPS) was performed on an axis ultra X-ray photoelectron spectrometer with an Al X-ray source operating at 250 W. The specimens were analyzed at an electron takeoff angle of 45°, and measured with respect to the surface plane. General survey scans (binding energy range 0–1100 eV, pass energy 188 eV) and high-resolution spectra (pass energy 29 eV) in the C1s, O1s, Si2p, N1s and I3d5 regions were recorded for the copolymer films.

Atomic force microscopy (AFM) was measured by scanning probe microscope (CSPM5500A, Being Nano-Instruments, Ltd.,

China) in tapping mode, in order to investigate the surface morphology of the block copolymer films. Samples were imaged at 3 μm × 3 μm magnifications using a nanosensor silicon tip.

Water contact angle (WCA) measurements (JC2000D contact angle meter from Shanghai Zhongchen Equipment Ltd., China) were carried out to evaluate the surface wettability of copolymer films by measuring the static contact angle between the film surface and demineralized water drops (ca. 5 μL). Advancing and receding contact angles were measured by increasing and decreasing the drop volume. The data presented were the average of five measurements.

2.5. Assessment of antimicrobial properties

The antimicrobial property of the crosslinked copolymer films was assessed with an agar plating method according to the reference [36], and this method was also adopted to evaluate organic silicone resin with QAS [6,9]. For these experiments, initial bacteria concentration was approximately 10^5–10^6 CFU/mL. 200 μL of initial bacteria was added on the nutrient agar plates and ensured the uniform distribution on the surface. The copolymer film coated aluminum sheets were placed slowly on the agar plates with the coated side directly contacted with the agar surface. The plates were inverted and incubated for 24 h at 37 °C. Inhibition of microbial growth around the coated aluminum sheets was evaluated visually from digital images taken after 24 h of incubation. For different bacteria, a transparent inhibition zone surrounding the coated specimen was designated as "+" for antimicrobial response.
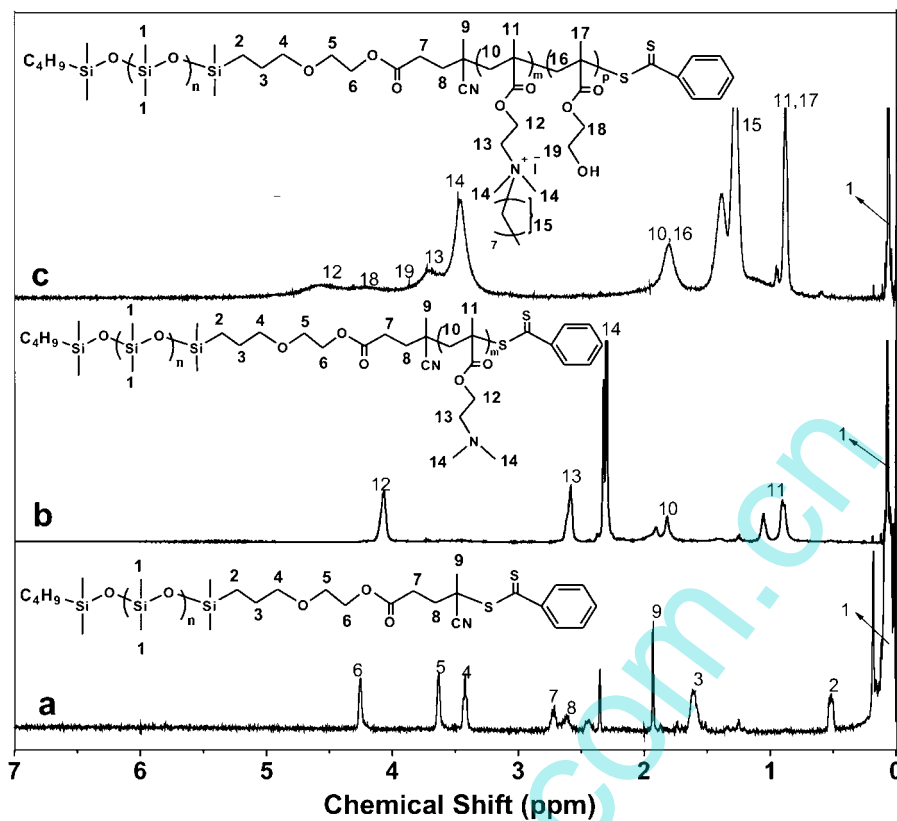
Fig. 1. ^{1}H NMR spectra of (a) PDMS-CTA, (b) PDMS-*b*-PDMAEMA, and (c) PDMS-*b*-QPDMAEMA-*b*-PHEMA.

Conversely, if films showed no inhibition zone, the antimicrobial response was given the designation "−".

3. Results and discussion

3.1. Synthesis of PDMS-b-QPDMAEMA copolymers

Fig. 1(a) and (b) shows the ^{1}H NMR spectra of PDMS-CTA and a purified PDMS-*b*-PDMAEMA sample, respectively. The characteristic peaks of PDMAEMA block appeared at 2.32 ppm, 2.58 ppm and 4.08 ppm, indicating that PDMS-*b*-PDMAEMA block copolymer was synthesized successfully. The molecular weights derived from the ^{1}H NMR spectra ($M_{n,NMR}$) were calculated according to the signal integrations of the protons from the methyl groups in Si(CH_3)$_2$ and the oxygen-methylene groups of PDMAEMA. The monomer conversion of DMAEMA via RAFT polymerization could reach above 60%, estimated from the ^{1}H NMR spectra. Table 1 summarizes the conversion and relative molecular weight of the prepared block copolymers.

The GPC traces show sharp and unimodal peaks in Fig. 2 (PDI < 1.27), and the relevant values are listed in Table 1. The copolymer molecular weights measured by ^{1}H NMR and GPC were consistent with each other.

The quaternization reaction between tertiary amino groups in PDMS-*b*-PDMAEMA and *n*-octyliodide proceeded to prepare PDMS-*b*-QPDMAEMA. Compared with the ^{1}H NMR spectra in Fig. 1(b) and (c), almost 100% of the tertiary amino groups in PDMAEMA blocks have been converted into QAS groups in the quaternization reaction. The proton peaks of dimethyl groups attached to the tertiary amine shift from 2.31 ppm to 3.47 ppm. Meanwhile, the signals of methylene groups attached to nitrogen atom at 2.59 ppm shift to 3.72 ppm, and characteristics for long alkyl chain appeared at 1.19–1.49 ppm. Besides, after quaternization reaction,

the polarity of block copolymers increased due to the electrostatic interaction of cationic groups.

Many researchers found that antimicrobial activity of polymers increased with molecular weight in a certain range, over which decreased sharply due to the hindrance of the functional groups through the bacteria cell membrane [5]. The molecular weight of the prepared copolymers in the present research was obtained in a controlled manner (in range of 17 kDa–50 kDa), and the brush structure was estimated with high density cationic groups (40–100 units/mol), therefore, promising properties are expected for biomedical antibacterial materials.

3.2. Thermal behaviors of the block copolymers

DSC thermograms of PDMS-*b*-PDMAEMA and PDMS-*b*-QPDMAEMA with different contents are shown in Fig. 3. The
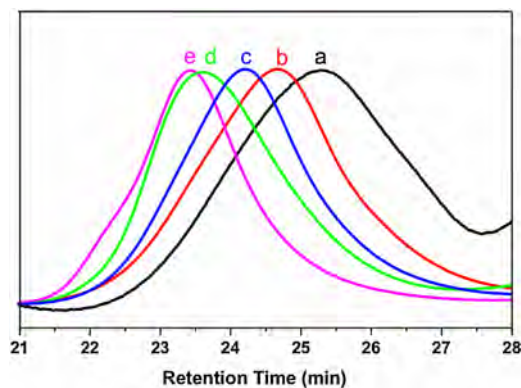

Fig. 2. GPC traces of (a) PDMS-CTA, (b) PDMS-*b*-PDMAEMA$_{40}$, (c) PDMS-*b*-PDMAEMA$_{60}$, (d) PDMS-*b*-PDMAEMA$_{80}$, and (e) PDMS-*b*-PDMAEMA$_{100}$.
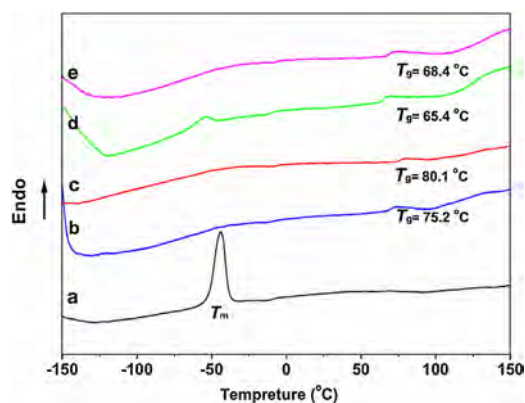
Fig. 3. DSC thermograms of the block copolymers: (a) PDMS-b-PDMAEMA$_{40}$, (b) PDMS-b-QPDMAEMA$_{40}$, (c) PDMS-b-QPDMAEMA$_{60}$, (d) PDMS-b-QPDMAEMA$_{80}$, and (e) PDMS-b-QPDMAEMA$_{100}$ (glass transition temperature T_g and melting temperature T_m indicated).

PDMS block exhibited a sharp peak of melting temperature (T_m) around −43.3 °C, which was evident in PDMS-b-PDMAEMA$_{40}$ (Fig. 3(a)). The absence of T_m in most quaternized copolymers, except for PDMS-b-QPDMAEMA$_{80}$, could be attributed to the counter ions groups, which affected the mobility of the copolymer chains in molecular packing and therefore hindered crystallization [31]. Additional T_gs associated with QPDMAEMA blocks were detected for all copolymers in the second heating runs, i.e. PDMS-b-QPDMAEMA$_{40}$ (75.2 °C), PDMS-b-QPDMAEMA$_{60}$ (80.1 °C), PDMS-b-QPDMAEMA$_{80}$ (65.4 °C), and PDMS-b-QPDMAEMA$_{100}$ (68.4 °C), and it was worth noting that the effect of QPDMAEMA content on T_g was not straightforward. As we know, counter ions are polar groups, which could increase the values of T_g, while the flexible alkyl side chains favor rearrangement of molecules and decrease the values of T_g. The polar groups were dominated for PDMS-b-QPDMAEMA$_{40}$ and PDMS-b-QPDMAEMA$_{60}$, and the values of T_g increased with the rise of counter ions amount in QPDMAEMA block. For PDMS-b-QPDMAEMA$_{80}$, the value of T_g decreased and T_m reappeared, which may be attributed to the flexible alkyl side chains in a proper content to favor the rearrangement of molecules.

3.3. Chemical compositions of the block copolymer films

The contents of carbon, oxygen, silicon, nitrogen, and iodide elements estimated from XPS are collected in Table 2. As we can see, the elemental ratios Si/N of PDMS-b-QPDMAEMA film surfaces were lower than those in the copolymers, and the smallest ratio of Si/N element was found in film PDMS-b-QPDMAEMA$_{60}$. PDMS was prone to migrate toward the surface due to its flexibility and low surface energy, however, the migration was somewhat limited by the increased content of QPDMAEMA. The significant discrepancy of Si/N ratio was relevant to the morphology evolvement detected by AFM in next section.

The high resolution XPS spectra of the N1s for block copolymer films are shown in Fig. 4. The results indicated that the presence of N1s peaks were resolved into C—N$^+$ and C—N, which appeared at 402.4 eV and 399.6 eV, respectively, and the percentages of C—N$^+$ and C—N were also shown in Fig. 4. Practically, in view of the total content of N element (Table 1), the higher percentages of C—N$^+$ were found on the film surfaces of PDMS-b-QPDMAEMA$_{60}$ and PDMS-b-QPDMAEMA$_{100}$. Considering the almost complete conversion of tertiary amino groups into QAS detected in ^{1}H NMR result, it is assumed that C—N was mainly generated from the crosslinker, which was consistent with the content used for crosslinking in
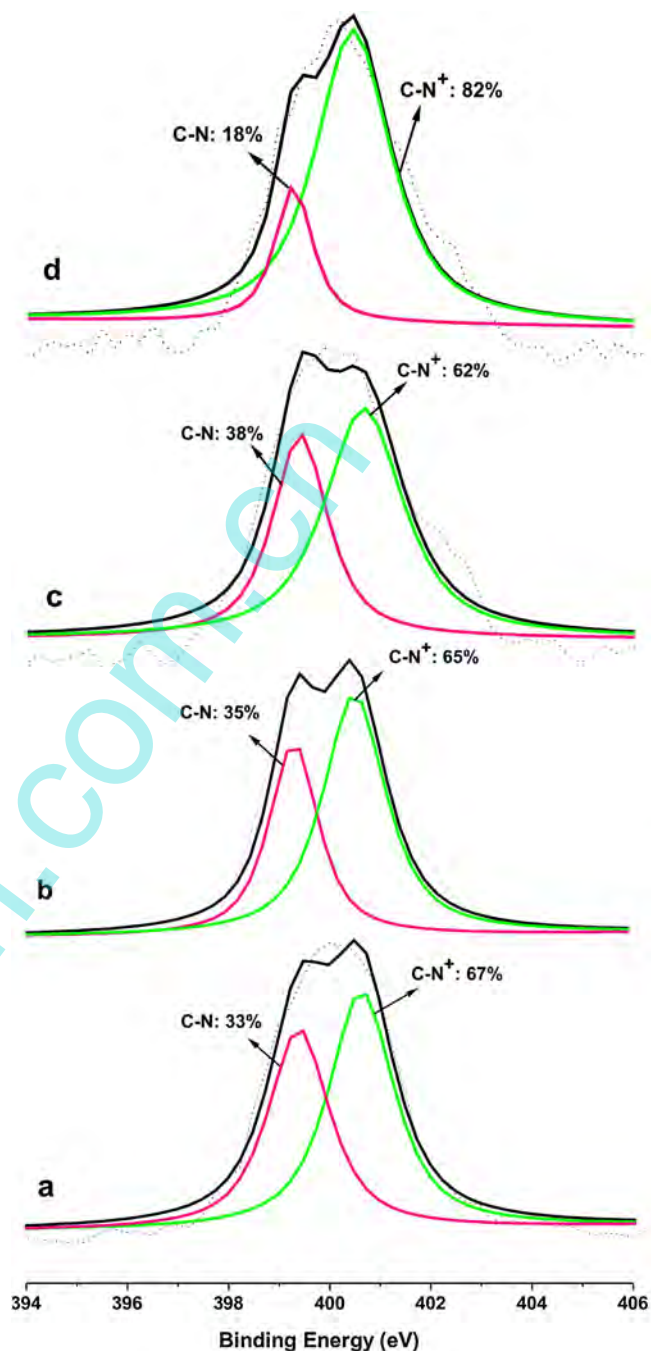

Fig. 4. High resolution XPS spectra of N1s for block copolymer films (a) PDMS-b-QPDMAEMA$_{40}$, (b) PDMS-b-QPDMAEMA$_{60}$, (c) PDMS-b-QPDMAEMA$_{80}$, and (d) PDMS-b-QPDMAEMA$_{100}$.

experiments. It is expected of course that the increased content of N$^+$ on surface would give rise to obvious antimicrobial activity.

3.4. Morphology of the copolymer films

Fig. 5 illustrates the copolymer films surface topography witnessed by AFM. The surface morphology evolved from "hole" to "bump" with the increased content of QPDMAEMA, presenting variation of roughness average in range of 1.18–3.88 nm (indicated as S_a in Fig. 5). Moreover, the diameter of round domains in both topography and phase images was getting smaller with the increased content of QPDMAEMA, i.e. the average diameter of the round domains about 200 nm was observed in PDMS-b-QPDMAEMA$_{40}$,

Table 2
Atomic percentage of the copolymer surface measured by XPS.

Sample	C1s (%)	O1s (%)	Si2p (%)	N1s (%)	I3d5 (%)	Si/N[a]	Si/N[b]
PDMS-*b*-QPDMAEMA$_{40}$	62.3	19.9	10.6	7.3	0	1.5/1	2.7/1
PDMS-*b*-QPDMAEMA$_{60}$	67.5	17.2	5.3	9.2	0.8	0.6/1	1.8/1
PDMS-*b*-QPDMAEMA$_{80}$	68.6	16.8	5.5	7.7	1.5	0.7/1	1.4/1
PDMS-*b*-QPDMAEMA$_{100}$	65.2	18.4	7.8	7.2	1.4	1.1/1	1.1/1

[a] Referring to the ratio on the copolymer film surface.
[b] Referring to the ratio in copolymer estimated from the content.

while the smaller domains with about 40 nm in average diameter were displayed by PDMS-*b*-QPDMAEMA$_{60}$. The incompatibility of PDMS and QPDMAEMA blocks in the copolymers was fundamental for microphase separation. In the formation process copolymer films, the PDMS block was prior to precipitate from acetonitrile, and the selectivity of solvent toward different blocks could affect the morphology. Besides, from the Si/N ratios listed in Table 2, it indicated the enrichment of QPDMAEMA on the film surfaces, that is, the migration of PDMS segments was restricted by both of the increased QPDMAEMA content and the cross-linked network
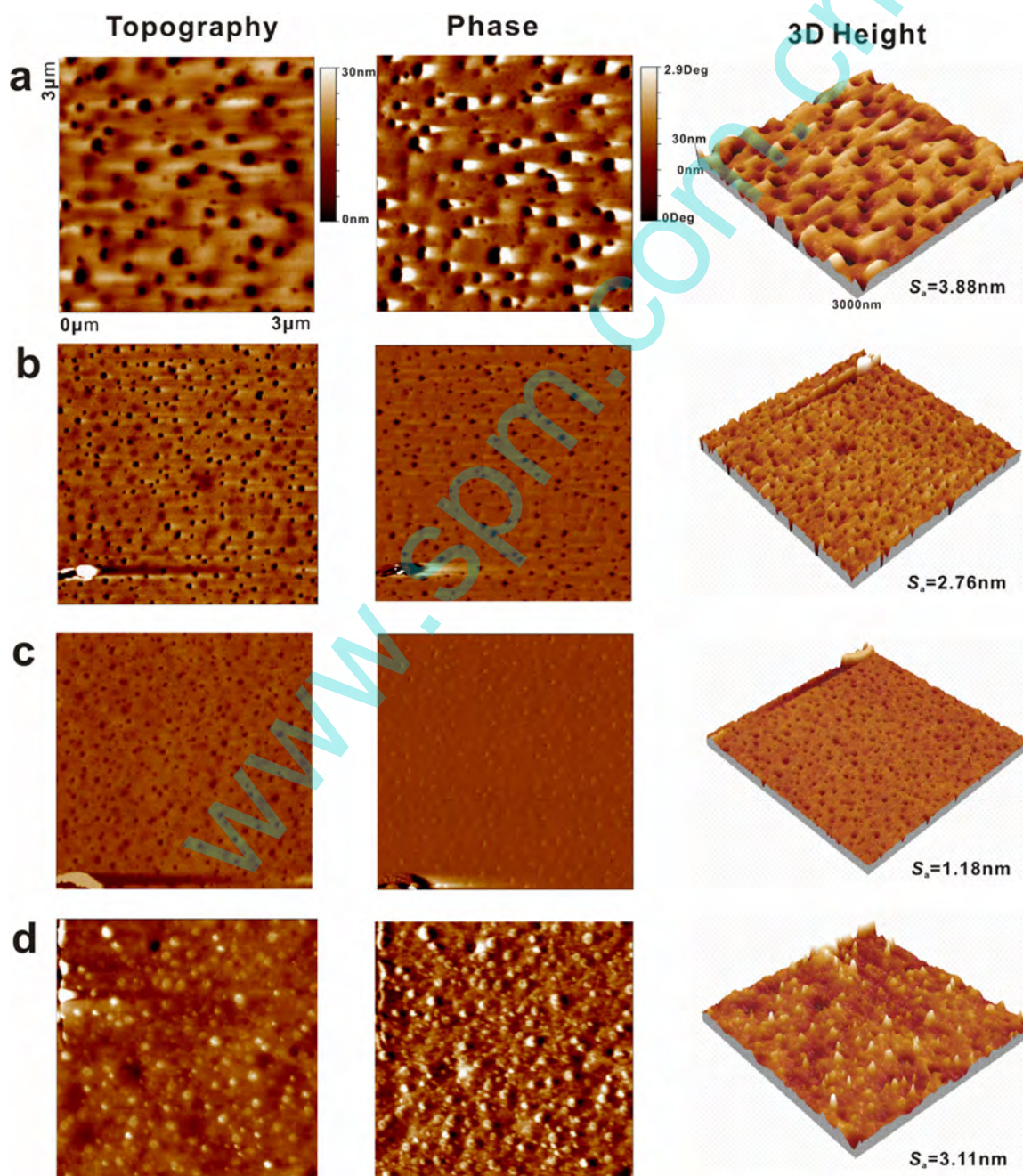

Fig. 5. AFM topography, phase images and 3D height of block copolymer films over a scope of 3 μm × 3 μm (a) PDMS-*b*-QPDMAEMA$_{40}$, (b) PDMS-*b*-QPDMAEMA$_{60}$, (c) PDMS-*b*-QPDMAEMA$_{80}$, and (d) PDMS-*b*-QPDMAEMA$_{100}$.
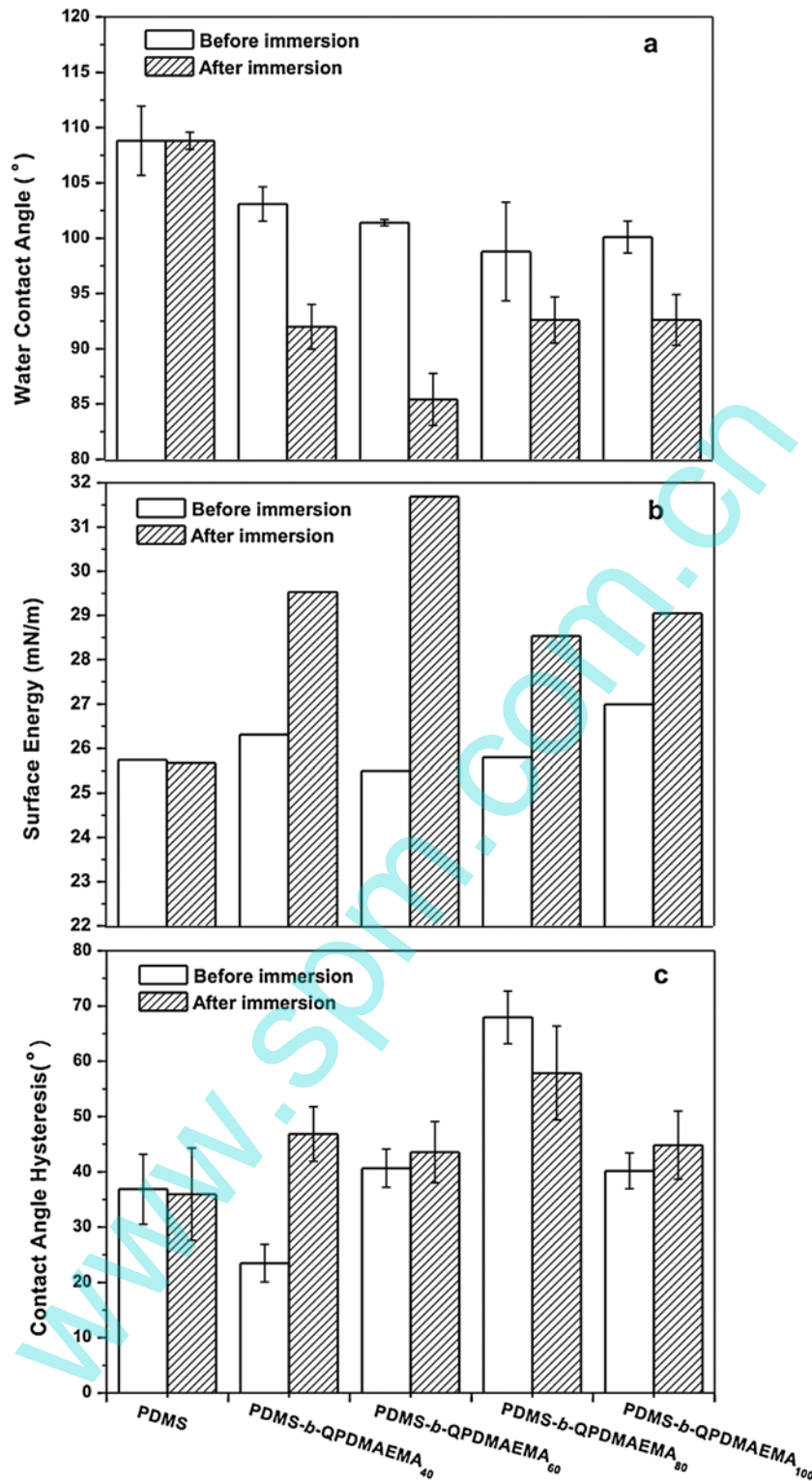
Fig. 6. Wettability of PDMS and block copolymer films (a) water contact angles, (b) surface energy, and (c) contact angle hysteresis.

of the copolymer films, a similar phenomenon had been reported elsewhere [37]. Consequently, it is speculated that the darker round domains in the phase images were attributed to PDMS-rich domains. Considering the XPS results in combination, microphase separation generated special composition and heterogeneous morphologies on copolymer film surface, which was bound to affect antimicrobial activity.

Furthermore, the morphologies of PDMS-b-QPDMAEMA$_{40}$ and PDMS-b-QPDMAEMA$_{100}$ films showed relatively larger phase contrasts than the other two samples. The surface morphology resulted from complex interactions among various parameters, such as temperature of curing, solvent, and content ratio of different blocks. The evolvements of topography and roughness derived from different migration rate of individual segment to the air/surface and
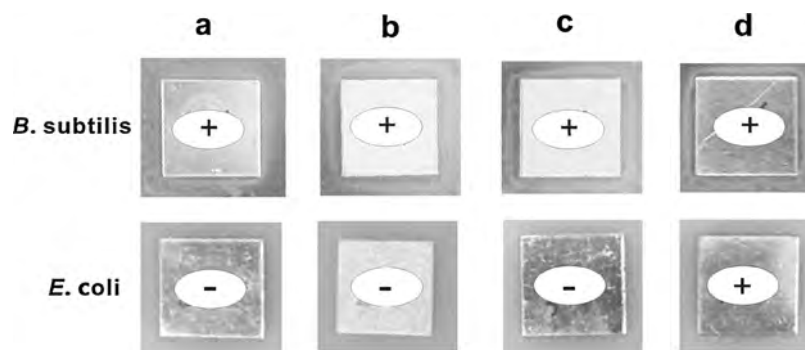
Fig. 7. Antimicrobial activity of block copolymer films (a) PDMS-*b*-QPDMAEMA$_{40}$, (b) PDMS-*b*-QPDMAEMA$_{60}$, (c) PDMS-*b*-QPDMAEMA$_{80}$, and (d) PDMS-*b*-QPDMAEMA$_{100}$.

fraction of each segment in the curing process. Intermolecular ionic interactions of QAS groups could provide additional thermodynamic driving force for microphase separation. Besides, the intramolecular actions between alkyl side chains and positively charged groups in QAS may also promote microphase separation, which is an assumption in other reports [6,9,38]. These factors resulted in the distinct microphase separation of PDMS-*b*-QPDMAEMA$_{40}$ and PDMS-*b*-QPDMAEMA$_{100}$.

3.5. Wettability of the block copolymer films

Fig. 6(a) shows that WCA of the copolymer films decreased with the increased content of QPDMAEMA before immersing in water, which was seemingly due to the cationic groups in QPDMAEMA. PDMS film was obtained through crosslinking and measured as control. The WCA and surface energy of PDMS film remained constant even after immersed in water for 24 h, while for the PDMS-*b*-QPDMAEMA films, the most reduction of WCA could reach 20° after immersing in water. The results were presented as expected that the surface wettability was increased because of the migration of QAS groups. Surface energy values of the block copolymers films are 26.3 mN/m, 25.5 mN/m, 25.8 mN/m, and 27.0 mN/m, respectively, with the increasing order of QPMAEMA content (shown in Fig. 6(b)). After immersion in water, the values of surface energy increased dramatically, which were also mainly dominated by the migration of QAS groups toward the surface. Theoretically, the variation of surface energy indicated the discrepancy of antimicrobial activity to some extent, and will be discussed in the follow-up section. The water contact angle hysteresis (CAH) provided a measurement of the stability for the film surface upon exposure to water [9,39]. Block copolymer films with QPDMAEMA resulted in a visible change in morphology and/or surface composition upon exposure to water, and the films exhibited larger CAH than pure PDMS film due to the existence of hydrogen bond between cationic group and water (Fig. 6(c)). Higher values of CAH also indicated the surface instability due to the variations of chemical composition and morphology [9], and this may improve the antimicrobial properties of block copolymer films to some extent. In addition, values of CAH rose with the increase of QPDMAEMA content, except for sample PDMS-*b*-QPDMAEMA$_{100}$ before contacting with water, and the change trend was exactly opposite to the variation of film roughness, i.e. CAH for PDMS-*b*-QPDMAEMA$_{40}$ (S_a = 3.88 nm) was 23°, while that for PDMS-*b*-QPDMAEMA$_{80}$ (S_a = 1.18 nm) was 68°. It is speculated that the existence of water on the film surface would provide a thermodynamic driving force for reorganization of QAS groups, in order to maximize molecular interactions between QAS groups and water molecules. These results are expected the reorganization of QAS groups on film surfaces could improve antimicrobial performances.

3.6. Antimicrobial activity of the block copolymer films

The antimicrobial performances of the copolymer films were investigated by visual observation. Fig. 7 displays the results obtained from the agar plating method. Transparent inhibition zones around each coated specimen indicated that all copolymer films had antimicrobial activity to *B. subtilis*, while the effect on *E. coli* was not distinct. Previous results had also shown that QAS tended to be more effective toward Gram-positive bacteria than Gram-negative bacteria [11]. Nevertheless, the QAS groups were tethered with the copolymers possessed relatively higher molecular weight, and a certain content of the QAS alkyl side chains on the film surface tended to fold back and the positively charged nitrogen atoms would be exposed in humid environment [7], which may hinder the penetration of alkyl chains toward cell membranes in the bacterial culturing condition [9,40].

Surface morphology seemingly exhibits no straightforward relationship with the antimicrobial properties, but the prominent role it plays in microorganism adhesion behaviors has been noticed [41–43]. Compared with the surface roughness and topography of the block copolymers, the film of PDMS-*b*-QPDMAEMA$_{40}$ had the largest roughness value (S_a = 3.88 nm). Consequently the QAS groups on the heterogeneous surface could sufficiently interfere with bacteria by the increased contact area, resulting in more excellent antimicrobial activity. Relatively, the block copolymer PDMS-*b*-QPDMAEMA$_{100}$ showed higher and broader-spectrum antimicrobial activity compared with other samples. Although further investigation was required, the migration of QAS groups to surface was easier from the "bump" morphology, and there was also a more migration probability for PDMS-*b*-QPDMAEMA$_{100}$ due to the highest QAS content, both of which made cationic amine groups effectively bind to the outer surface of the bacteria cell structures. Chemical composition of the surfaces contributed to the antimicrobial properties as well, and the similar results had been reported [38,44]. Therefore, with regard to structure-antimicrobial relationships, the surfaces with more content of N$^+$ and heterogeneous surface morphology are expected to present better antimicrobial activity.

In addition, antimicrobial activities are also required to take structures of bacteria into account [11,45,46]. Negative bacterium is wrapped with two kinds of cell membranes, while Gram-positive bacterium has only a single thin cell membrane, which is easily subject to be attacked by QAS groups. The antimicrobial mechanism depends on both of the particular copolymer surface and bacterial species. The investigation on surface composition, morphology, and the combined effect on antimicrobial activity, is expected to promote further antibacterial research.

4. Conclusion

A series of block copolymers PDMS-*b*-QPDMAEMA with different content of quaternary ammonium salt groups were synthesized via RAFT polymerization and quaternization. Thermal behaviors of the copolymers changed after quaternization reaction and were affected by the counter ions and flexible alkyl side chains in QPDMAEMA blocks. The elemental ratios of Si/N and morphology of the copolymer film surfaces were dependent on the content of QPDMAEMA blocks. In addition, with the variation content of QPDMAEMA, the reduction of WCA values reached up to 20° after block copolymer films immersed in water. In brief, the well-defined copolymers could generate special composition and unique morphology on film surfaces, which allows greater insight into the structure-antimicrobial activity relationship. The antimicrobial activity was highly dependent on the surfaces with heterogeneous morphology and higher N$^+$ content, and PDMS-*b*-QPDMAEMA$_{100}$ showed higher and broader-spectrum antimicrobial activity.

Acknowledgment

References

[1] A. Asadinezhad, I. Novak, M. Lehocky, V. Sedlarík, A. Vesel, I. Junkar, P. Sáha, I. Chodak, An *in vitro* bacterial adhesion assessment of surface-modified medical-grade PVC, Colloids Surf. B 77 (2010) 246–256.

[2] J. Liang, J.R. Owens, T.S. Huang, S.D. Worley, Biocidal hydantoinylsiloxane polymers. IV. *N*-halamine siloxane-functionalized silica gel, J. Appl. Polym. Sci. 101 (2006) 3448–3454.

[3] B.P. Mowery, S.E. Lee, D.A. Kissounko, R.F. Epand, R.M. Epand, B. Weisblum, S.S. Stahl, S.H. Gellman, Mimicry of antimicrobial host-defense peptides by random copolymers, J. Am. Chem. Soc. 129 (2007) 15474–15476.

[4] Y. Liu, Y. Liu, X.H. Ren, T.S. Huang, Antimicrobial cotton containing *N*-halamine and quaternary ammonium groups by grafting copolymerization, Appl. Surf. Sci. 296 (2014) 231–236.

[5] E.R. Kenawy, S.D. Worley, R. Broughton, The chemistry and applications of antimicrobial polymers: a state-of-the-art review, Biomacromolecules 8 (2007) 1359–1384.

[6] P. Majumdar, J. He, E. Lee, A. Kallam, N. Gubbins, S.J. Stafslien, J. Daniels, B.J. Chisholm, Antimicrobial activity of polysiloxane coatings containing quaternary ammonium-functionalized polyhedral oligomeric silsesquioxane, J. Coat. Technol. Res. 7 (2010) 455–467.

[7] Y.W. Liu, C. Leng, B. Chisholm, S. Stafslien, P. Majumdar, Z. Chen, Surface structures of PDMS incorporated with quaternary ammonium salts designed for antibiofouling and fouling release applications, Langmuir 9 (2013) 2897–2905.

[8] W. Fortuniak, U. Mizerska, J. Chojnowski, T. Basinska, S. Slomkowski, M.M. Chehimi, A. Konopacka, K. Turecka, W. Werel, Polysiloxanes with quaternary ammonium salt biocidal functions and their behavior when incorporated into a silicone elastomer network, J. Inorg. Organomet. Polym. 21 (2011) 576–589.

[9] P. Majumdar, E. Lee, N. Gubbins, S.J. Stafslien, J. Daniels, C.J. Thorson, B.J. Chisholm, Synthesis and antimicrobial activity of quaternary ammonium-functionalized POSS (Q-POSS) and polysiloxane coatings containing Q-POSS, Polymer 50 (2009) 1124–1133.

[10] G. Sauvet, S. Dupont, K. Kazmierski, J. Chojnowski, Amphiphilic block and statistical siloxane copolymers with antimicrobial activity, J. Appl. Polym. Sci. 75 (2000) 1005–1012.

[11] C.Z. Chen, N.C. Beck-Tan, P. Dhurjati, T.K. Dyk, R.A. LaRossa, S.L. Cooper, Quaternary ammonium functionalized poly(propylene imine) dendrimers as effective antimicrobials: structure-activity studies, Biomacromolecules 1 (2000) 473–480.

[12] Y. Sui, X.L. Gao, Z.N. Wang, C.J. Gao, Antifouling and antibacterial improvement of surface-functionalized poly(vinylidene fluoride) membrane prepared via dihydroxyphenylalanine-initiated atom transfer radical graft polymerizations, J. Membr. Sci. 394–395 (2012) 107–119.

[13] D.D. Yao, Y.J. Guo, S.G. Chen, J.N. Tang, Y.M. Chen, Shaped core/shell polymer nanoobjects with high antibacterial activities via block copolymer microphase separation, Polymer 54 (2013) 3485–3491.

[14] Y.T. Joo, K.H. Jung, M.J. Kim, Y.S. Kim, Preparation of antibacterial PDMAEMA-functionalized multiwalled carbon nanotube via atom transfer radical polymerization, J. Appl. Polym. Sci. 127 (2012) 1508–1518.

[15] H. Murata, R.R. Koepsel, K. Matyjaszewski, A.J. Russell, Permanent, non-leaching antibacterial surfaces. 2. How highdensity cationic surfaces kill bacterial cells, Biomaterials 28 (2007) 4870–4879.

[16] Y. Chen, P.A. Wilbon, Y.P. Chen, J. Zhou, M. Nagarkatti, C.P. Wang, F.X. Chu, A.W. Dechob, C.B. Tang, Amphipathic antibacterial agents using cationic methacrylic polymers with natural rosin as pendant group, RSC Adv. 2 (2012) 10275–10282.

[17] P. Majumdar, B. Mayo, J. Kim, C. Gallagher-Lein, E. Lee, N. Gubbins, B.J. Chisholm, The utilization of specific interactions to enhance the mechanical properties of polysiloxane coatings, J. Coat. Technol. Res. 7 (2010) 239–252.

[18] P. Ferreiral, A. Carvalho, T.R. Correia, P.A. Bernardo, I.J. Correia, P. Alves, Functionalization of polydimethylsiloxane membranes to be used in the production of voice prostheses, Sci. Technol. Adv. Mater. 14 (2013), 055006.

[19] R.F. Brady, I.L. Singer, Mechanical factors favoring release from fouling release coatings, Biofouling 15 (2000) 73–81.

[20] Y.J. Sun, S.L. Guo, G.C. Walker, C.J. Kavanagh, G.W. Swain, Surface elastic modulus of barnacle adhesive and release characteristics from silicone surfaces, Biofouling 20 (2004) 279–289.

[21] A.C. Schneid, E.W. Roesch, F. Sperb, U. Matte, N.P. da Silveira, Silver nanoparticle-ionic silsesquioxane: a new system proposed as an antibacterial agent, J. Mater. Chem. B 2 (2014) 1079–1086.

[22] A. Goyal, A. Kumar, P.K. Patra, S. Mahendra, S. Tabatabaei, P.J. Alvarez, G. John, P.M. Ajayan, In situ synthesis of metal nanoparticle embedded free standing multifunctional PDMS films, Macromol. Rapid Commun. 30 (2009) 1116–1122.

[23] O. Girshevitz, Y. Nitzan, C.N. Sukenik, Solution-deposited amorphous titanium dioxide on silicone rubber: a conformal, crack-free antibacterial coating, Chem. Mater. 20 (2008) 1390–1396.

[24] H.J. Bai, H.L. Gou, J.J. Xu, H.Y. Chen, Molding a silver nanoparticle template on polydimethylsiloxane to efficiently capture mammalian cells, Langmuir 26 (2010) 2924–2929.

[25] Q. Tu, J.C. Wang, R. Liu, J. He, Y.R. Zhang, S.F. Shen, J. Xu, J.J. Liu, M.S. Yuan, J.Y. Wang, Antifouling properties of poly(dimethylsiloxane) surfaces modified with quaternized poly(dimethylaminoethyl methacrylate), Colloids Surf. B 102 (2013) 361–370.

[26] A.J. Keefe, N.D. Brault, S.Y. Jiang, Suppressing surface reconstruction of superhydrophobic PDMS using a superhydrophilic zwitterionic polymer, Biomacromolecules 13 (2012) 1683–1687.

[27] S.W. Hu, X.Q. Ren, M. Bachman, C.E. Sims, G.P. Li, N.L. Allbritton, Tailoring the surface properties of poly(dimethylsiloxane) microfluidic devices, Langmuir 20 (2004) 5569–5574.

[28] D.T. Eddington, J.P. Puccinelli, D.J. Beebe, Thermal aging and reduced hydrophobic recovery of polydimethylsiloxane, Sens. Actuators B 114 (2006) 170–172.

[29] Y. Chen, M.Q. Niu, S. Yuan, H.N. Teng, Durable antimicrobial finishing of cellulose with QSA silicone by supercritical adsorption, Appl. Surf. Sci. 264 (2013) 171–175.

[30] X.M. Lian, F. Zhao, Y. Li, J. Wang, S.M. Li, H.Y. Zhao, Photophysical properties and self-assembly of triblock copolymer with complexes of positively charged PDMAEMA and oppositely charged chromophores, Polymer 53 (2012) 1906–1914.

[31] W. Zhao, P. Fonsny, P. FitzGerald, G.G. Warr, P. Sebastien, Unexpected behavior of polydimethylsiloxane/poly(2-(dimethylamino)ethyl acrylate) (charged) amphiphilic block copolymers in aqueous solution, Polym. Chem. 4 (2013) 2140–2150.

[32] S. Boileau, L. Bouteiller, A. Kowalewska, Telechelic polydimethylsiloxanes with terminal acetylenic groups prepared by phase-transfer catalysis, Polymer 44 (2003) 6449–6455.

[33] S.H. Thang, Y.K. Chong, R.T. Mayadunne, G. Moad, E. Rizzardo, A novel synthesis of functional dithioesters, dithiocarbamates, xanthates and Trithiocarbonates, Tetrahedron Lett. 40 (1999) 2435–2438.

[34] M.L. Wadley, K.A. Cavicchi, Synthesis of polydimethylsiloxane-containing block copolymers via reversible addition fragmentation chain transfer (RAFT) polymerization, J. Appl. Polym. Sci. 115 (2010) 635–640.

[35] T.H. Duong, C. Bressy, A. Margaillan, Well-defined diblock copolymers of poly(tert-butyldimethylsilyl methacrylate) and poly(dimethylsiloxane) synthesized by RAFT polymerization, Polymer 55 (2014) 39–47.

[36] A. Kugela, S. Stafslien, B.J. Chisholm, Antimicrobial coatings produced by tethering biocides to the coating matrix: a comprehensive review, Prog. Org. Coat. 72 (2011) 222–252.

[37] H.X. Fang, S.X. Zhou, L.M. Wu, Microphase separation behavior on the surfaces of PEG-MDI-PDMS multiblock copolymer coatings, Appl. Surf. Sci. 253 (2006) 2978–2983.

[38] P. Majumdar, E. Lee, N. Gubbins, D.A. Christianson, S.J. Stafslien, J. Daniels, L. VanderWal, J. Bahr, B.J. Chisholm, Combinatorial materials research applied to the development of new surface coatings XIII: an investigation of polysiloxane antimicrobial coatings containing tethered quaternary ammonium salt groups, J. Comb. Chem. 11 (2009) 1115–1127.

[39] P. Majumdar, E. Crowley, M. Htet, S.J. Stafslien, J. Daniels, L. VanderWal, B.J. Chisholm, Combinatorial materials research applied to the development of new surface coatings XV: an investigation of polysiloxane anti-fouling/fouling-release coatings containing tethered quaternary ammonium salt groups, ACS Comb. Sci. 13 (2011) 298–309.

[40] L.B. Rawlinson, S.M. Ryan, G. Mantovani, J.A. Syrett, D.M. Haddleton, D.J. Brayden, Antibacterial effects of poly(2-(dimethylaminoethyl)methacrylate) against selected Gram-positive and Gram-negative bacteria, Biomacromolecules 11 (2010) 443–453.

[41] L.C. Hsu, J. Fang, D.A. Borca-Tasciuc, R.W. Worobo, C.I. Moraru, Effect of micro- and nanoscale topography on the adhesion of bacterial cells to solid surfaces, Appl. Environ. Microbiol. 79 (2013) 2703–2712.

[42] N. Mitik-Dineva, J. Wang, R.C. Mocanasu, P.R. Stoddart, R.J. Crawford, E.P. Ivanova, Impact of nano-topography on bacterial attachment, Biotechnol. J. 3 (2008) 536–544.

[43] S.D. Puckett, P.P. Lee, D.M. Ciombor, R.K. Aaron, T.J. Webster, Nanotextured titanium surfaces for enhancing skin growth on transcutaneous osseointegrated devices, Acta Biomater. 6 (2010) 2352–2362.

[44] P.A. Fulmer, J.H. Wynne, Development of broad-spectrum antimicrobial latex paint surfaces employing active amphiphilic compounds, ACS Appl. Mater. Interfaces 3 (2011) 2878–2884.

[45] J.Y. Song, Y.J. Jung, I. Lee, J. Jang, Fabrication of pDMAEMA-coated silica nanoparticles and their enhanced antibacterial activity, J. Colloid Interface Sci. 407 (2013) 205–209.

[46] U. Mizerska, W. Fortuniak, J. Chojnowski, R. Hałasa, A. Konopacka, W. Werel, Polysiloxane cationic biocides with imidazolium salt (ImS) groups, synthesis and antibacterial properties, Eur. Polym. J. 45 (2009) 779–787.